nature electronics

ARTICLES

https://doi.org/10.1038/s41928-019-0206-5

Self-healing electronic skins for aquatic environments

Yue Cao[1,2,9], Yu Jun Tan[3,4,9], Si Li[3,4], Wang Wei Lee[3,4], Hongchen Guo[3,5], Yongqing Cai[6], Chao Wang[1*] and Benjamin C.-K. Tee[3,4,7,8*]

Gelatinous underwater invertebrates such as jellyfish have organs that are transparent, stretchable, touch-sensitive and self-healing, which allow the creatures to navigate, camouflage themselves and, indeed, survive in aquatic environments. Artificial skins that emulate such functionality could be used to develop applications such as aquatic soft robots and water-resistant human–machine interfaces. Here we report a bio-inspired skin-like material that is transparent, electrically conductive and can autonomously self-heal in both dry and wet conditions. The material, which is composed of a fluorocarbon elastomer and a fluorine-rich ionic liquid, has an ionic conductivity that can be tuned to as high as 10^{-3} S cm^{-1} and can withstand strains as high as 2,000%. Owing to ion–dipole interactions, it offers fast and repeatable electro-mechanical self-healing in wet, acidic and alkali environments. To illustrate the potential applications of the approach, we used our electronic skins to create touch, pressure and strain sensors. We also show that the material can be printed into soft and pliable ionic circuit boards.

Artificial electronic materials with skin-like capabilities have potential applications in soft robotics[1–4], human–machine interfaces[5–7] and healthcare[8–10]. Creating materials that can also function underwater could extend such applications to various aquatic and marine environments. Several approaches to create stretchable electronic materials have been reported[11–13], and recent biomimetic suction cups have illustrated the potential of underwater mechanical functionalities[14].

Developing materials that can self-heal in wet environments could potentially allow simpler repairs, leading to waste reduction and greater resilience[15,16]. Some self-healing devices require solvent and thermal treatment[17], and others use magnetic effects to self-heal[18]. Although these systems provide pathways towards self-healing devices, they require extrinsic stimuli or additional materials for healing.

For unobtrusive underwater exploration, materials with inherent optical transparency would also be desirable. However, conventional electrically conducting metals are opaque. A repeatedly self-healing electronic skin has been demonstrated that can heal autonomously under ambient environments, but the material was opaque owing to the incorporation of metal particles within a hydrogen-bond-filled polymer matrix[19]. A stretchable polymer that is self-healable underwater based on hydrogen bonding was recently designed, but it needs to incorporate liquid-state metals to enable conductivity, which also leads to opaque regions[20]. Another way to make a self-healable underwater stretchable material using dipole–dipole interactions has been proposed[21], but the material is an electrical insulator. To make it electrically conducting, silver flakes were incorporated, which again resulted in an opaque composite.

Using transparent conductive polymers, highly transparent electronic skins can be engineered[22]. Tough hydrogels containing electrolytes have been used to create various electronic devices thanks to the stretchability, transparency and conductivity of the material[5,23,24]. Although hydrogel materials have tunable mechanical properties and can allow self-healing capabilities with the addition of reversible bonding[25,26], varying conditions of humidity can greatly affect their electro-mechanical properties. For example, hydrogels in dry environments can lose water content over time, and in wet environments can absorb water and swell (Supplementary Fig. 1a,b). Protective coatings on the hydrogels can be used, but may not last longer than 48 h[4] and create additional complexities when developing electronic applications for long-term use. Sufficiently robust and self-healable conductive hydrogels could be designed for environments with modulated humidity, but may not be suitable for devices that are operated in ambient or underwater environments for long periods of time.

A key challenge for aquatic-based skin electronics is to develop a single material system that combines transparency, stretchability, self-healing and submergibility. In the natural world, jellyfish (a type of gelatinous underwater invertebrate) possess such properties, which allow them, for example, to self-camouflage and to communicate optically with each other[27,28].

In this Article, we report submersible self-healing electronic skin sensors inspired by transparent jellyfish[28]. We combine an amorphous polymer with a chemically compatible ionic species to a create gel-like, aquatic, stretchable and self-healing electronic skin, which we term 'GLASSES' (Fig. 1a). GLASSES can self-heal through highly reversible ion–dipole interactions, which allows for intrinsically conductive, transparent, stretchable and self-healing capabilities in aquatic conditions. Previous approaches to creating self-healing materials using dynamic bonds have been based on hydrogen bonds and metal–ligand coordination[19,29–31].

[1]Key Lab of Organic Optoelectronics & Molecular Engineering, Department of Chemistry, Tsinghua University, Beijing, China. [2]Department of Chemistry, University of California Riverside, Riverside, California, USA. [3]Department of Materials Science and Engineering (MSE), National University of Singapore, Singapore, Singapore. [4]Biomedical Institute for Global Health and Research (BIGHEART), National University of Singapore, Singapore, Singapore. [5]Graduate School for Integrative Sciences and Engineering, National University of Singapore, Singapore, Singapore. [6]Institute Of High Performance Computing (IHPC), Agency for Science Technology and Research, Singapore, Singapore. [7]Department of Electrical and Computer Engineering (ECE), National University of Singapore, Singapore, Singapore. [8]Institute of Materials Research and Engineering (IMRE), Agency for Science Technology and Research, Singapore, Singapore. [9]These authors contributed equally: Yue Cao, Yu Jun Tan. *e-mail: chaowangthu@tsinghua.edu.cn; benjamin.tee@nus.edu.sg

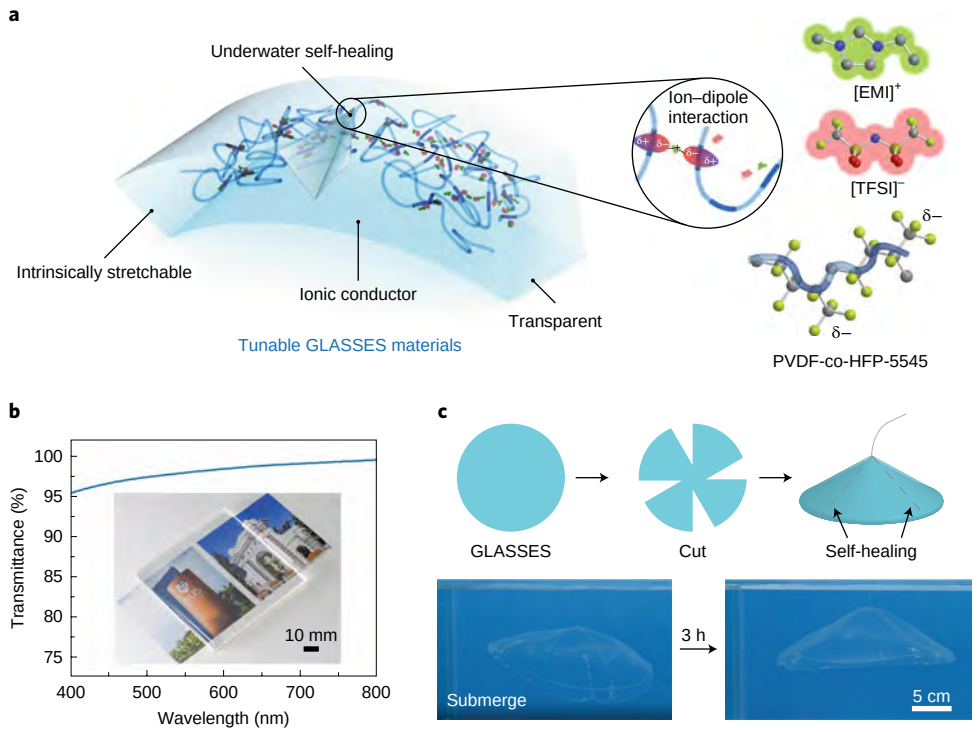

Fig. 1 | Design of a gel-like, aquatic, stretchable and self-healing electronic skin (GLASSES). a, Schematic illustration of the self-healing of the conductive polymer. A stretchable polymer network with high chain dipole moment interacts with a mobile ionic liquid to form GLASSES. The polymer chains self-heal through highly reversible ion–dipole interactions. **b**, Transmittance spectrum of 30 wt% EMITFSI with a film thickness of 0.2 mm. An average transmittance over 98% was recorded in the visible range (400–800 nm). Inset: photograph of the film on a glass slide. **c**, Self-healed GLASSES submerged in water for 3 h retains its shape, self-healing capability and transparency.

Such approaches make it challenging for the materials to operate under aquatic conditions because water molecules, which can act as hydrogen donor/acceptors, ligands and polar solvents, can bind to most of the hydrogen-bonding sites or metal–ligand coordination sites, thereby substantially decreasing their binding strength. Consequently, such self-healing polymers will swell and lose healing capability in aqueous environments.

Synthesis and characteristics of GLASSES

GLASSES consists of two components: a highly polar fluoro-elastomer and a fluorine-rich ionic liquid. We used an amorphous elastomer[29] with a very high dipole moment, poly(vinylidene fluoride-co-hexafluoropropylene) P(VDF-HFP), together with 1-ethyl-3-methylimidazolium bis(trifluoromethylsulfonyl) imide ($[EMI]^+$ $[TFSI]^-$ or EMITFSI) as the ionic liquid. The ionic liquid is stable and does not evaporate over time owing to its negligible vapour pressure[32].

The GLASSES fluoro-elastomer consists mostly of carbon–fluorine (C–F) bonds. The ionic liquid interacts with the polymer chains via ion-dipole interactions. C–F bonds are very poor hydrogen donors and acceptors owing to the high electronegativity of fluorine and the strong electrostatic nature of the C–F bond. As a result, both the fluoro-elastomers and the fluorine-rich ionic liquids have weak interactions with water molecules. Therefore, water environments will minimally perturb the ion-dipole interactions, making the GLASSES composite hydrophobic. This is in contrast to self-healing materials that contains many carbon–nitrogen (C–N) bonds and carbon–oxygen (C–O) bonds, which interact strongly with water molecules. This design allows our material to self-heal underwater.

The dipoles of the GLASSES polymer chains strongly interact with the cations in the ionic liquid. In addition, the steric hindrance provided by the CF_3 pendant group in HFP provides mobile ions with more free volume, giving rise to higher ionic conductivity and concomitant self-healing capability. Moreover, the high miscibility of the ionic liquid with the polymer renders the GLASSES composite highly transparent, with an average transmittance of over 98% under visible light wavelengths (Fig. 1b).

Critically, we found that submerging GLASSES in water did not change its shape and appearance (Fig. 1c), compared to other self-healing materials where noticeable swelling was observed (Supplementary Fig. 1c–d). Moreover, the self-healed interfaces in GLASSES remained intact underwater. We found that the EMITFSI used in GLASSES retained well within the polymer matrix when submerged in water (Supplementary Fig. 1e and Supplementary Table 1). This result is consistent with the estimation from our density functional theory (DFT) calculations.

In the DFT calculations, we compared our GLASSES material to a previously described self-healing ionogel[29] that used the same base polymer P(VDF-HFP), but with a hydrophilic ionic liquid 1-ethyl-3-methylimidazolium trifluoromethanesulfonate (EMIOTf). The DFT calculations show much stronger interactions between the P(VDF-HFP) with EMITFSI than with EMIOTf (Supplementary Note 1). Moreover, the water molecule interacts more readily with EMIOTf (Supplementary Note 2), and the interaction between the P(VDF-HFP) moiety and the EMITFSI is also stronger in the presence of water molecules compared with EMIOTf (Supplementary Note 3). The DFT results indicate that EMITFSI possesses stronger ionic interactions with P(VDF-HFP), and much weaker interactions with water. Thus, these findings help to explain the stability of our GLASSES material in water.

Our experimental results further demonstrated that GLASSES can retain its properties underwater even after 12 h, but the electro-mechanical and optical properties of P(VDF-HFP)-EMIOTf

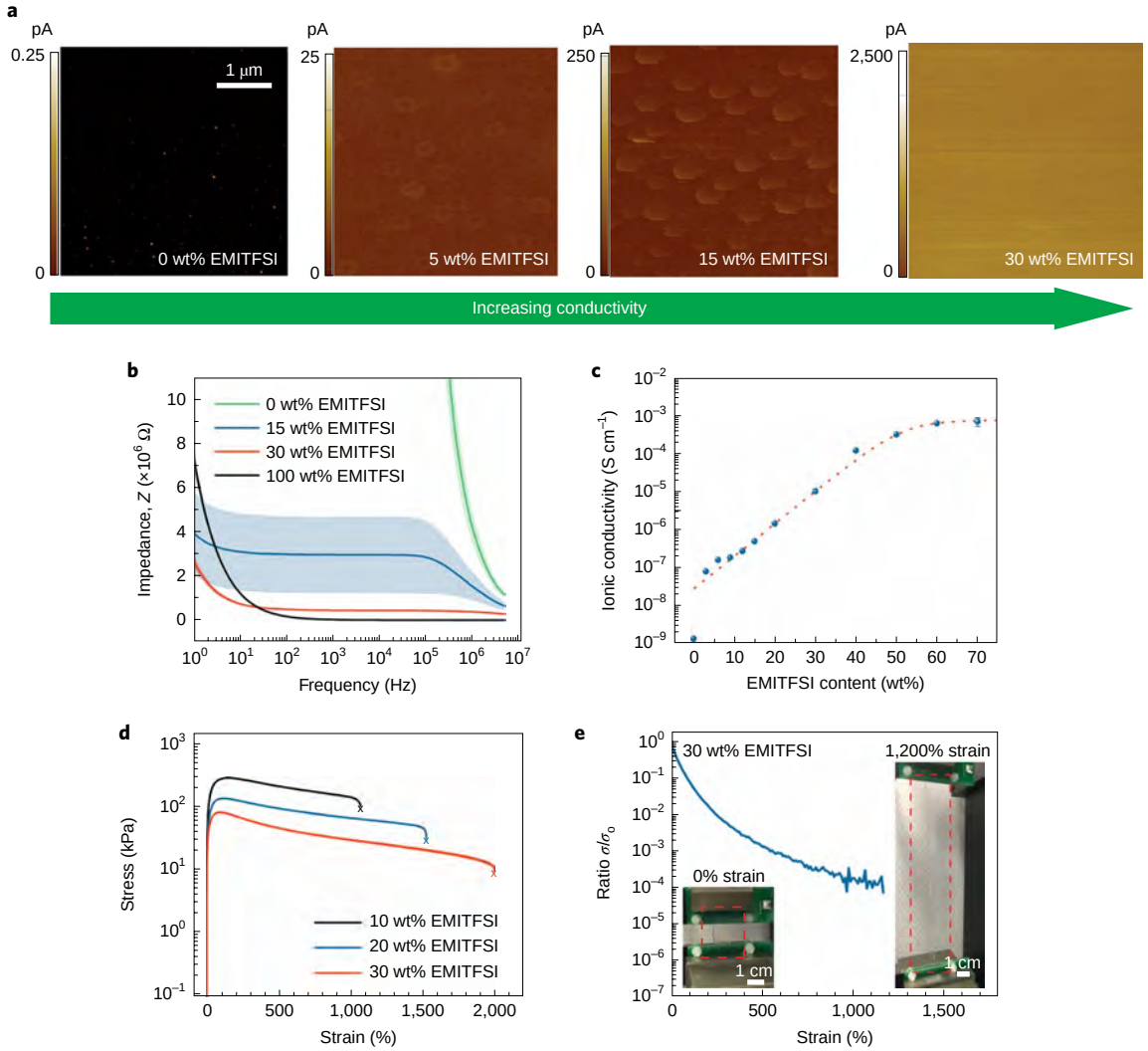

Fig. 2 | Tunable electrical and mechanical properties of the GLASSES material. a, Conductive atomic force microscopy results, showing the transition from insulating (0 wt% EMITFSI) to discrete micrometre-sized droplets of EMITFSI (5 wt%, 15 wt% EMITFSI) to a percolating phase of EMITFSI (30 wt% EMITFSI) in the polymer network. **b**, Influence of frequency on the impedance of materials. The measurements were repeated on three samples and the error bars shown in shaded areas represent the standard deviation. **c**, Influence of EMITFSI concentrations on the conductivity of the conductive polymer. The measurements were reproduced on three samples and the error bars represent the standard deviation. **d**, Stress–strain curves showing the increase in stretchability but decrease in strength with increasing concentration of EMITFSI in GLASSES. **e**, Conductivity decreases with the increase in strain. Insets show the photos of the material at 0% and 1,200% strain.

changed substantially after being immersed in water (Supplementary Fig. 1f, Supplementary Table 2, Supplementary Note 4). As the ionic liquids contain the same cation $[EMI]^+$, the main difference between EMITFSI and EMIOTf arises from the water solubility of their anions. $[TFSI]^-$ is a poor hydrogen bond acceptor owing to the delocalization of its negative charge and steric hindrance (Supplementary Note 4). Therefore, GLASSES can be used as a conductive polymer under wet conditions.

Electro-mechanical properties

The electrical conductivity and mechanical properties of GLASSES are highly tunable by varying the proportion of ionic liquid to the polymer. Using conductive atomic force microscopy, we observed that there is a transition from discrete micrometre-sized droplets to a fully percolating phase of ionic liquid in the polymer network (Fig. 2a). The electrical conductivity of the material increases by six orders of magnitude from 10^{-9} S cm^{-1} to 10^{-3} S cm^{-1} as the EMITFSI concentration increased from 0 wt% to 70 wt% (Fig. 2b,c and Supplementary Fig. 2). Materials bereft of EMITFSI has low conductivity because the insulating P(VDF-HFP) hinders the ionic transport. On the other hand, GLASSES with a high content of EMITFSI form a homogeneous conducting medium where the ions are highly mobile. The ionic conductivity of the materials increases with temperature as the ions drift more rapidly (Supplementary Fig. 3).

We showed that the material exhibited higher strain failure point, lower Young's modulus, and lower maximum tensile stress as the content of EMITFSI increases from 10 wt% to 30 wt% (Fig. 2d). With EMITFSI content higher than about 30 wt%, the ionogels were viscous and cannot hold their shapes over time. When strained to 50% elongation, GLASSES materials with 10 wt% to 40 wt% EMITFSI can return to their original lengths. A GLASSES material with 50 wt% EMITFSI is elastic up to 30% strain (Supplementary Fig. 4a–e).

At higher strains, the strain-induced changes are not fully reversible. However, even after being stretched to 1,000% strain, the GLASSES ionogel could gradually return to twice its original

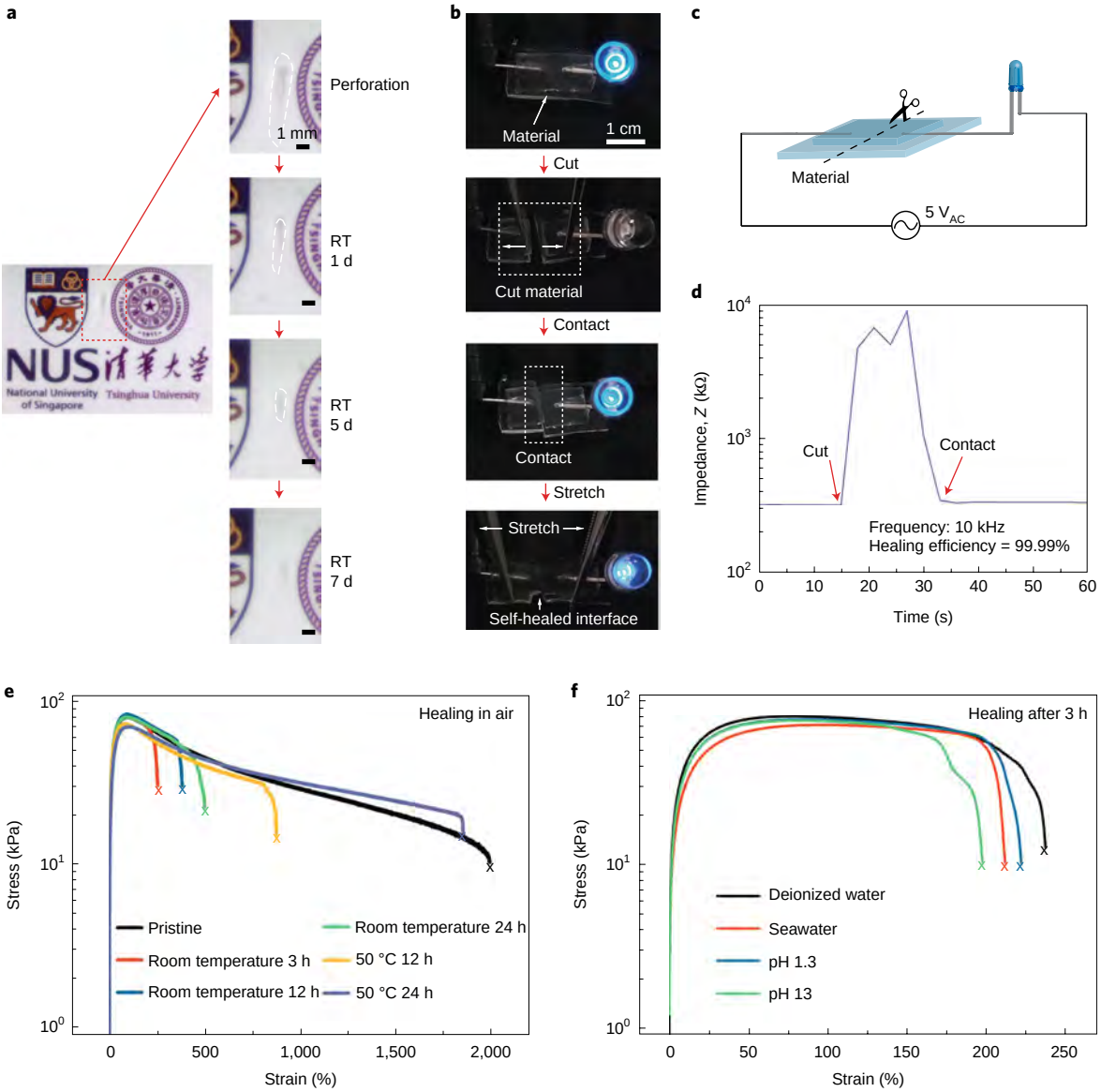

Fig. 3 | Electro-mechanical self-healing abilities. a, Microscope images showing that the material heals autonomously after being cut at room temperature (RT). Dotted lines indicate damaged regions. **b**–**d**, Demonstration of the healing process of conductivity for the material with a light-emitting diode (LED). The electrical properties (impedance) healed completely upon contact, with initial mechanical healing observed when gently stretched. **e**, Typical stress–strain curves of original and healed samples for different healing times and temperature for the 30 wt% EMITFSI materials. **f**, Stress–strain curves of healed 30 wt% EMITFSI samples in different water environments for 3 h. The material exhibited similar healing ability in acidic water, basic water and seawater.

length within 2 h (Supplementary Fig. 4f). The material with 30 wt% EMITFSI exhibited a Young's modulus of 0.21 MPa, which is comparable to conventional soft rubbers. It is also noteworthy that the polymer possessed a larger modulus at higher loading rates (Supplementary Fig. 4g), which is typical for supramolecular rubbery materials. The conductivity of GLASSES decreased upon stretching (Fig. 2e). This may be due to the optically observable strain-induced crystallization of the polymer during stretching (Supplementary Fig. 5), which reduces the mobility of the ions in the material.

We observed that GLASSES retained its electro-mechanical properties even after full submersion in water. We compared its properties to a self-healing ionogel using a previously described hydrophilic ionic liquid, EMIOtf[29] . We found that GLASSES maintained its properties after submerging for 12 h, but the ionogel made using hydrophilic EMIOtf had noticeably different physical properties(Supplementary Table 2). These differences occurred because the hydrophobicity of EMITFSI (discussed earlier and in Supplementary Note 4) increases the diffusion barrier of the ions out of the ionogel, thereby preserving the GLASSES material's physical properties in water.

Electro-mechanical self-healing

We further demonstrated the autonomous electro-mechanical self-healing abilities of GLASSES by creating a visible cut on the material. The material subsequently heals under ambient conditions without adding extraneous solvents or materials, as indicated in Fig. 3a and Supplementary Video 1. The speed of healing

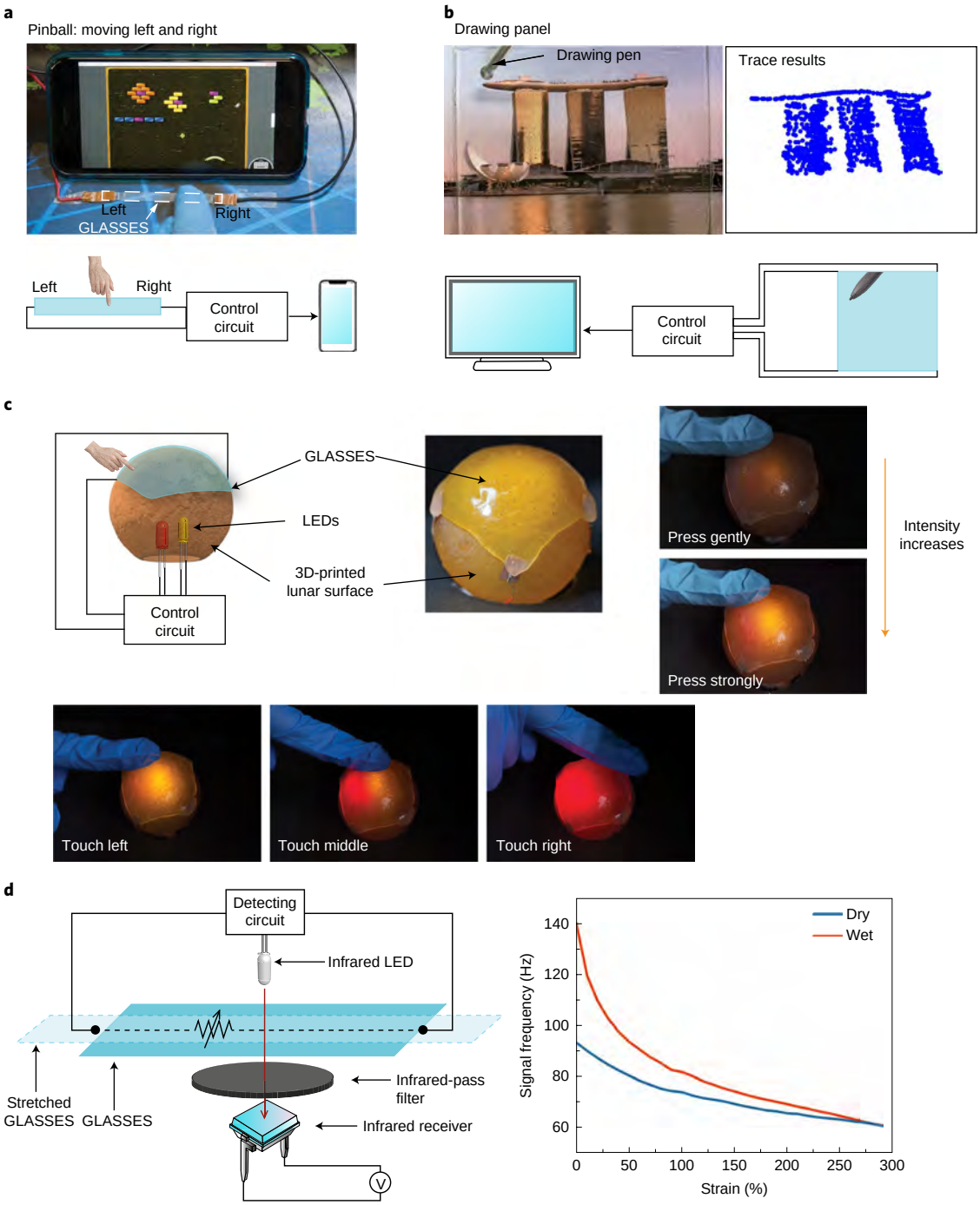

Fig. 4 | Touch, pressure and strain sensors fabricated from GLASSES. a, Demonstration and schematic drawing of the 'pinball' game, played by controlling the direction of finger 'swipes' on the one-dimensional GLASSES touch bar. **b**, Demonstration and schematic drawing of a drawing pad in dry and wet conditions, where the tracing of a picture is controlled by the pen's 'drawing' on a two-dimensional touchpad. **c**, Schematic drawing showing how a conformable pressure sensor is configured by covering a spherical 'lunar' surface with a piece of GLASSES. The LED light varied between different touching areas, and its light intensity varies with the pressure. **d**, Demonstration of an infrared communication system in air and water, and the signal–strain plot showing that the transmitted signal carrying information (frequency) is dependent on the strain.

depends on the severity of damage and the content of EMITFSI in the materials (Supplementary Fig. 6a and Supplementary Table 3). The material self-heals electrically when cut halves are placed back together upon slight contact, as exhibited in Fig. 3b–d. Repeatable, autonomous healing of its conductivity was tested and the healing efficiency was 90.7% after ten cuts using the ceramic knife (Supplementary Fig. 6b–c).

We define the mechanical self-healing efficiency as the proportion of toughness restored relative to the original toughness (the area under the stress–strain curve), because this method considers the restoration of both the stress and the strain[19]. For all samples, the GLASSES materials maintained their Young's modulus and followed the same tensile stress curves as shown in Fig. 3e. The restoration of mechanical properties of the materials is evident without any

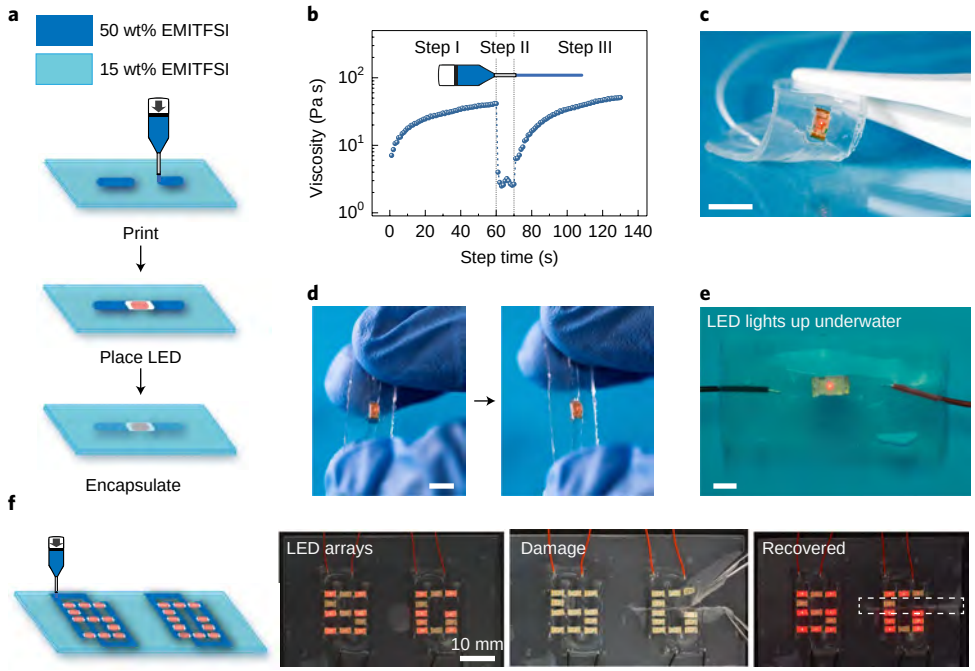

Fig. 5 | Soft, stretchable, transparent, self-healing PCB. a, Fabrication diagram showing the printing process of soft PCB. **b**, Graph showing the viscosity change of the ink before (step I), during (step II) and after (step III) printing. The ink exhibited a thixotropic behaviour that is favourable for extrusion-based 3D printing. **c**, Photograph showing the printed flexible PCB device. Scale bar, 5 mm. **d**, Photograph of the soft PCB being stretched to 30% strain. Scale bar, 5 mm. **e**, The device can also work underwater (water dyed blue). Scale bar, 2 mm. **f**, The PCB can be scaled up to a larger array of LEDs. The soft PCB self-healed after sustaining damage (highlighted region in box).

external stimulus but can be enhanced by elevated temperatures. The material recovers by about 43.9% after 24 h under room temperature conditions, and recovered to 99.1% after 24 h when healed at 50 °C.

Intriguingly, the material can heal even when submerged in various aqueous environments, such as in deionized water, sea water, or in extremely acidic and basic solutions, as shown in Fig. 3f. After healing for three hours in deionized water, the materials can be stretched to 200% strain, with a healing efficiency of 22.6%. When the samples were healed in seawater, pH 1.3 solution and pH 13 solutions for three hours, the healing efficiencies were 18.8%, 20.9% and 17.4% respectively. The underwater healing speed was faster at 50 °C (Supplementary Fig. 7). The sample recovered 33.8% of its toughness in 3 h. The self-healing performance under various environments is due to the fluorinated polymers, which are known to be stable under different conditions, such as salty, different pH, and so on. In addition, the hydrophobicity of the ionic liquid synergistically shielded it against the water molecules.

The self-healing efficiencies of the material in the air and underwater are summarized in Supplementary Table 4. The GLASSES material was observed to retain self-healing performance underwater. In contrast, the hydrophilic ionogel[28] irreversibly lost its self-healing capability upon submersion in water because the ionic liquid leaked out from the polymer when submerged (discussed above and in Supplementary Note). We observed some aging effects at the GLASSES cut interface (Supplementary Fig. 8), where the polymer chains at the aged surface reoriented and form self-complementary bonds over time.

Compared to current self-healing stretchable materials, GLASSES material has several more useful properties, as shown in Supplementary Fig. 9. Furthermore, the material properties can be tailored because the concentration of EMITFSI has an effect on the mechanical properties and on the transport properties of the ions. EMITFSI acts as a plasticizer that substantially reduces the glass transition temperature, T_g, of the materials (Supplementary Fig. 10), increases the segmental mobility of the polymer and simultaneously enhances the conductivity. GLASSES is stable over a long time with no observed changes in its form and properties. Self-healing is efficient because the active ion-dipole entanglement network is available at clean interfaces whether dry or wet. P(VDF-HFP) polymer chains are mobile in EMITFSI, which also facilitates self-healing (Supplementary Fig. 11a). Polymer fibres can bridge across the damaged interfaces when the clean cut surfaces are placed together (Supplementary Fig. 11b).

GLASSES as electronic skins

We used the GLASSES materials in one-dimensional and two-dimensional touch sensors to demonstrate their potential for electronic skin applications (Fig. 4a,b and Supplementary Video 2–3). We observed that the conductivity of the material remained stable from a frequency of around 100 Hz to a plateau around 100 kHz, where the material behaved purely resistively (Supplementary Fig. 12). In all the demonstrated applications, we standardized the testing frequency at 10 kHz within the plateau region. We first demonstrated touch sensing through a surface-capacitive system[5] using GLASSES as a screen (Supplementary Figs. 13–16). Unlike an ionic hydrogel-based touch sensor[5], which is inherently humidity-sensitive, no change in the appearance and properties of GLASSES was observed over time.

The touch positions of a GLASSES-based touch sensor were calibrated before use (Supplementary Fig. 15). As expected, it can function when wet (Supplementary Figs. 17–18). We further illustrate a conformable, transparent touch and pressure sensor (Fig. 4c, Supplementary Fig. 19 and Supplementary Video 4). We wrapped GLASSES onto a 3D-printed rough spherical lunar-like surface, with red and yellow LEDs connected to the output of the control circuit and placed inside the sphere. The output of the amplifying circuit varies with the touch areas of the sensor, and the LEDs light

up on demand, where light radiates through the materials. The output signal changes according to the force applied by the finger, because the interface deformation of GLASSES and fingertip will change the surface-capacitive path. The intensity of light varies with the force of pressing on the GLASSES, illustrating its potential use as a pressure sensor.

In addition, we made use of its high transparency by incorporating GLASSES into an opto-electronic communication system[33], akin to intraspecific communications by sea jellies using bioluminescence[27]. The GLASSES film is placed between an infrared LED and a receiver, as illustrated in Fig. 4d and Supplementary Fig. 20. The film was then stretched, which resulted in an increase in resistance. This change modulated the frequency of a ring oscillator circuit that was connected to the transparent GLASSES strain sensor, which in turn changed the emitting frequency of the infrared LED (Supplementary Video 5). We measured the frequency changes in both wet and dry conditions and observed that in both instances, the signal frequencies decrease with strain. The measured frequencies were higher when wet than when dry.

To demonstrate machine–machine communications using GLASSES, we constructed an artificial 'jellyfish' using a transparent balloon (Supplementary Video 6). A strip of GLASSES adheres to the bottom of the balloon's surface, and an infrared LED was placed within the balloon cavity. An opaque tube was used to ensure the infrared light transmits through the GLASSES material. An infrared receiver was aligned underneath the position of the GLASSES and wrapped onto the external balloon surface. The display on the phone showed the physical status of the balloon. We demonstrated that as the balloon continues to inflate, signal transmission occurs even when the GLASSES material was submerged in water as the balloon continues to inflate. Furthermore, we formed an artificial jellyfish umbra using GLASSES and affixed a yellow LED within it to demonstrate the potential of our material for unobtrusive underwater surveillance devices. Moving the transparent 'jellyfish' around unlit did not disrupt the normal behaviour of small crustaceans, but when the LED is switched on, an immediate reaction was elicited (Supplementary Video 7).

Traditional rigid printed circuit boards (PCBs) electrically connect components using conductive tracks on a rigid, non-conductive substrate. Taking advantage of the printability of the GLASSES material, we designed and fabricated a fully transparent and self-healable soft ionic PCB. The 50 wt% EMITFSI and 15 wt% EMITFSI are analogous to the conventional conductive tracks and the non-conductive substrate, respectively. A polar solvent was used to assist in the printing of the conductive ink (see Methods). Figure 5a and Supplementary Fig. 21 show the printing of the ink onto a 15 wt% EMITFSI substrate. The ink is suitable for printing because it is thixotropic (it flows only under stress) (Fig. 5b).

By encapsulating the soft PCB (one LED patterned across the 50 wt% EMITFSI) with 15 wt% EMITFSI materials, we demonstrated a pliable circuit whereby the LED lights up in ambient and aquatic conditions after being stretched in pristine and healed scenarios (Fig. 5c–e, Supplementary Fig. 22 and Supplementary Video 8). This printing method for PCB based on GLASSES can be scaled up to larger arrays, with a pattern of LEDs forming alphabetic symbols 'SG' (Fig. 5f). The LEDs lit up again after the soft GLASSES PCB was cut, owing to the subsequent intrinsic electro-mechanical healing at the cut interface.

Conclusions

We have developed a transparent gel-like composite material system with tunable mechanical and electronic properties. Our material can be formed into stretchable electronic skins that can autonomously self-heal in both dry and wet conditions. We fabricated a touch, pressure and strain sensor platform to demonstrate the sensory capabilities of our material. The high optical transparency of our material suggests uses in emerging opto-electronic human–machine and machine–machine communication interfaces for unobtrusive underwater exploration[34].

Methods

Materials synthesis. The material synthesis and preparations followed the typical steps used in preparing fluoroelastomer composites[21]. First, acetone was used to dissolve PVDF-co-HFP-5545 (3 M Dyneon Fluoroelastomer FE) and the required amounts of the ionic liquid (1-ethyl-3-methylimidazolium bis(trifluoromethylsulfonyl)imide (EMITFSI; Solvionic)) and the mixture was stirred at room temperature (>4 h) to obtain a well dispersed solution. Next, a dried film was formed in a Petri dish by drying the acetone in a vacuum oven (at 70 °C for 24 h). Compression moulding of the samples was performed to obtain sample sheets (1.0 mm thick).

The samples were then used for testing of mechanical, electrical properties and self-healing properties. Optical images were taken using optical microscopes (Keyence). Optical transmittance values were measured on films made from 1 g per 5 ml anhydrous acetone dried on top of glass slides (50 mm × 75 mm). Conductive atomic force microscopy measurements were conducted on similarly processed films (about 0.2 mm thick).

DFT calculations. First-principles calculations were performed by using the Vienna ab initio simulation package (VASP) package. Van der Waals interactions were considered within the DFT-D2 scheme. All the structures are relaxed until the forces exerted on each atom was less than 0.005 eV Å^{-1}. The interactions of molecules were simulated and modelled with periodic boundaries conditions. The thickness of the vacuum region was set greater than 10 Å to avoid the molecule interacting with its image. The first Brillouin zone was sampled with single point and a kinetic energy cut-off of 400 eV was adopted.

Electro-mechanical characterization. The conductivities of the GLASSES were visualized using conductive atomic force microscopy. The ionic conductivities of the materials were computed from the complex impedance plots measured by an impedance meter (Zurich Instruments; MFIA) at room temperature, over the frequency range from 1 Hz to 5 MHz with an alternating-current sine wave amplitude of 300 mV. The bulk resistance (R_b) of the materials was fitted from the Nyquist plot using the Z-view software from the intercept on the real-axis at a high frequency. The ionic conductivity (σ) was then calculated using the relation $\sigma = L/(R_b \times A)$, where L and A represent the thickness and area of the ionic conductor, respectively.

Mechanical testing was performed using an Instron 5942 instrument. Unless otherwise noted, tensile experiments were performed at room temperature (25 °C) at a strain rate of 5 mm min^{-1} for both stretching and relaxing rate. Each mechanical test was repeated with three individual samples of each ionic liquid content. Healing experiments were performed at either room temperature or 50 °C, and gently bringing the cut pieces back into contact. We measured the conductivity versus strain rate using a linear stretcher (Newmark) coupled with the impedance meter and collected the data electronically using a custom LabView script.

Differential scanning calorimetry measurements from −50 °C to 150 °C with a heating speed of 5 °C min^{-1} were performed using a PerkinElmer DSC 8000. Transmission data were recorded on an Ocean Optics HR2000CG-UVNIR spectrometer.

Electro-mechanical self-healing tests. To observe the time-lapse self-healing process, the material was cut using a sharp knife and then observed under a microscope. The self-healing of electro-mechanical properties test was conducted by cutting the material into two pieces and then putting the freshly cut surface back into contact. To verify the underwater self-healing capability, the samples were put into a Petri dish filled with deionized water, and cut into halves with a fresh razor blade. Then, the cut surfaces were gently placed together underwater, and subsequently left in water at room temperature to permit healing. Healing in different media including acidic water, basic water and seawater followed the same procedure. The samples to behealed at 50 °C underwater were transferred into a 60-ml glass bottle in a hot water bath. Mechanical tests took place after the designated healing time.

Touch panel. Copper foils were used as terminal electrodes to the one-dimensional (5 mm × 40 mm) and the two-dimensional GLASSES materials (40 mm × 40 mm), connected to the input of an amplifying circuit. Data Acquisition (NI cDAQ-9178) and Labview were used to read and process the signals of the circuit. Touch position can be determined by comparing the amplitudes of the signal.

Conformable pressure sensor. A hollow lunar model was 3D printed using a 3D printer (Aureus PLUS; material PIC 100). A piece of square material (40 mm × 40 mm) was put on the surface of the lunar model, where the material conforms on the uneven surface. Amplifying circuits were connected to the terminal electrodes of the material. The output of the circuits was used to drive the red and yellow LEDs that were inserted in the lunar model.

Infrared signal transmission and opto-electronic communication system. 30 wt% EMITFSI material was connected as the feedback resistance of the 5-stage oscillator. An infrared LED was placed above the material, and driven by the output signals via an output buffer. At the other side of the material, a photon receiver DP101 covered by an infrared filter is used to receive the signals from the infrared LED. For the opto-electronic communication system, a strip of material is bonded onto a transparent balloon, and the infrared source is guided by an opaque tube to pass through the material only. Similarly, the material was connected as the feedback resistance of a 5-stage oscillator.

Soft PCB. 50 wt% EMITFSI was printed using a dispenser system (Musashi) onto a 15 wt% EMITFSI substrate (less conductive substrate). The ink for printing consists of 50 wt% EMITFSI: acetone in around 1:1.6 ratio. Thixotropic properties of the ink were studied using a rheometer (DHR; TA Instruments). The test indicating the rheological properties of the ink during three phases of 3D printing: before printing (step I; 60 s; shear rate of 0.1 s^{-1}), during extrusion (step II; 10 s; shear rate of 50 s^{-1}), and after printed on a substrate (step III; 60 s; shear rate of 0.1 s^{-1})[35]. Materials with shear thinning properties (at step II) and recoverable viscosities after the shearing (step III) are thixotropic and suitable to be 3D printed via the extrusion-based method. SMD LEDs (KP-3216SURC) were put across two conductive tracks, which connected to an alternating-current power supply using silver-plated copper wire. The supply voltage amplitudes for a single LED and for the LED array were 20 V alternating voltage (V_{AC}) and 80 V_{AC}, respectively.

Data availability

The data that support the plots within this paper and other findings of this study are available from the corresponding author upon reasonable request.

Received: 15 August 2018; Accepted: 18 January 2019;
Published online: 15 February 2019

References

1. Larson, C. et al. Highly stretchable electroluminescent skin for optical signaling and tactile sensing. *Science* **351**, 1071–1074 (2016).
2. Bauer, S. et al. 25th Anniversary Article: a soft future: from robots and sensor skin to energy harvesters. *Adv. Mater.* **26**, 149–162 (2014).
3. Morin, S. A. et al. Camouflage and display for soft machines. *Science* **337**, 828–832 (2012).
4. Yuk, H., Zhang, T., Parada, G. A., Liu, X. & Zhao, X. Skin-inspired hydrogel–elastomer hybrids with robust interfaces and functional microstructures. *Nat. Commun.* **7**, 12028 (2016).
5. Kim, C.-C., Lee, H.-H., Oh, K. H. & Sun, J.-Y. Highly stretchable, transparent ionic touch panel. *Science* **353**, 682–687 (2016).
6. Wang, S. et al. Skin electronics from scalable fabrication of an intrinsically stretchable transistor array. *Nature* **555**, 83–88 (2018).
7. Tee, B. C. K. et al. Tunable flexible pressure sensors using microstructured elastomer geometries for intuitive electronics. *Adv. Funct. Mater.* **24**, 5427–5434 (2014).
8. Gao, W. et al. Fully integrated wearable sensor arrays for multiplexed in situ perspiration analysis. *Nature* **529**, 509–514 (2016).
9. Schwartz, G. et al. Flexible polymer transistors with high pressure sensitivity for application in electronic skin and health monitoring. *Nat. Commun.* **4**, 1859 (2013).
10. Chen, L. Y. et al. Continuous wireless pressure monitoring and mapping with ultra-small passive sensors for health monitoring and critical care. *Nat. Commun.* **5**, 1–10 (2014).
11. Lipomi, D. J. et al. Skin-like pressure and strain sensors based on transparent elastic films of carbon nanotubes.*Nat. Nanotechnol.* **6**, 788–792 (2011).
12. Sekitani, T., Zschieschang, U., Klauk, H. & Someya, T. Flexible organic transistors and circuits with extreme bending stability. *Nat. Mater.* **9**, 1015–1022 (2010).
13. Kim, K. S. et al. Large-scale pattern growth of graphene films for stretchable transparent electrodes. *Nature* **457**, 706–710 (2009).
14. Baik, S. et al. A wet-tolerant adhesive patch inspired by protuberances in suction cups of octopi. *Nature* **546**, 396–400 (2017).
15. Tan, Y. J., Wu, J., Li, H. & Tee, B. C. K. Self-healing electronic materials for a smart and sustainable future. *ACS Appl. Mater. Interfaces* **10**, 15331–15345 (2018).
16. Patrick, J. F., Robb, M. J., Sottos, N. R., Moore, J. S. & White, S. R. Polymers with autonomous life-cycle control. *Nature* **540**, 363–370 (2016).
17. Oh, J. Y. et al. Intrinsically stretchable and healable semiconducting polymer for organic transistors. *Nature* **539**, 411–415 (2016).
18. Bandodkar, A. J. et al. All-printed magnetically self-healing electrochemical devices. *Sci. Adv* **2**, e1601465 (2016).
19. Tee, B. C. K., Wang, C., Allen, R. & Bao, Z. An electrically and mechanically self-healing composite with pressure- and flexion-sensitive properties for electronic skin applications. *Nat. Nanotechnol.* **7**, 825–832 (2012).
20. Kang, J. et al. Tough and water-insensitive self-healing elastomer for robust electronic skin. *Adv. Mater.* **30**, 1706846 (2018).
21. Cao, Y. et al. A highly stretchy, transparent elastomer with the capability to automatically self-heal underwater. *Adv. Mater.* **30**, 1804602 (2018).
22. Lipomi, D. J. et al. Electronic properties of transparent conductive films of PEDOT:PSS on stretchable substrates. *Chem. Mater.* **24**, 373–382 (2012).
23. Keplinger, C. et al. Stretchable, transparent, ionic conductors. *Science* **341**, 984–987 (2013).
24. Sun, J.-Y., Keplinger, C., Whitesides, G. M. & Suo, Z. Ionic skin. *Adv. Mater.* **26**, 7608–7614 (2014).
25. Wirthl, D. et al. Instant tough bonding of hydrogels for soft machines and electronics. *Sci. Adv.* **3**, 1–10 (2017).
26. Taylor, D. L. & Het Panhuis, M. Self-healing hydrogels. *Adv. Mater.* **28**, 9060–9093 (2016).
27. Kaartvedt, S. et al. Social behaviour in mesopelagic jellyfish. *Sci. Rep.* **5**, 11310 (2015).
28. Johnsen, S. Transparent animals. *Sci. Am.* **282**, 80–89 (2000).
29. Cao, Y. et al. A transparent, self-healing, highly stretchable ionic conductor. *Adv. Mater.* **29**, 1605099 (2017).
30. Cordier, P., Tournilhac, F., Soulié-Ziakovic, C. & Leibler, L. Self-healing and thermoreversible rubber from supramolecular assembly. *Nature* **451**, 977–980 (2008).
31. Li, C.-H. et al. A highly stretchable autonomous self-healing elastomer. *Nat. Chem.* **8**, 618–624 (2016).
32. Earle, M. J. et al. The distillation and volatility of ionic liquids. *Nature* **439**, 831–834 (2006).
33. Tee, B. C. K. et al. A skin-inspired organic digital mechanoreceptor. *Science* **350**, 313–316 (2015).
34. Katzschmann, R. K., DelPreto, J., MacCurdy, R. & Rus, D. Exploration of underwater life with an acoustically controlled soft robotic fish. *Sci. Robot.* **3**, eaar3449 (2018).
35. Li, H., Tan, Y. J., Leong, K. F. & Li, L. 3D bioprinting of highly thixotropic alginate/methylcellulose hydrogel with strong interface bonding. *ACS Appl. Mater. Interfaces* **9**, 20086–20097 (2017).

Acknowledgements

B.C.-K.T. is grateful for the support of a National Research Foundation Fellowship by the Singapore National Research Foundation (NRF) Prime Minister's Office, and the National University of Singapore (NUS) Startup Grant. H.C.G. acknowledges support from a NUS NGS Scholarship. C.W. acknowledges support from NSFC grant no. 21890731. We thank J.Y. Sun for discussions and S. Wang, J. Tan, H. Li and W. Yan for access to testing equipment.

Author contributions

B.C.-K.T., C.W., Y.C., and Y.J.T. conceived and designed the experiments; Y.C., Y.J.T., S.L. and W.W.L. carried out experiments and collected the overall data; Y.C., Y.J.T. and H.C.G. contributed to materials fabrication and characterization. S.L., W.W.L. and Y.J.T. performed electrical properties characterization and worked on sensors demonstration. S.L. and Y.J.T. worked on transparent and self-healable soft PCB. Y.Q.C. contributed the DFT calculations. Y.J.T., B.C.-K.T., Y.C., S.L. and C.W. analysed all the data and co-wrote the paper. All authors discussed the results and commented on the manuscript.

Competing interests

The authors declare no competing interests.

Additional information

Supplementary information is available for this paper at https://doi.org/10.1038/s41928-019-0206-5.

Reprints and permissions information is available at www.nature.com/reprints.

Correspondence and requests for materials should be addressed to C.W. or B.C.-K.T.

Publisher's note: Springer Nature remains neutral with regard to jurisdictional claims in published maps and institutional affiliations.